CISTER
Research Centre in
Real-Time & Embedded
Computing Systems

Journal Paper

Energy Savings and Emissions Reduction of BEVs at an Isolated Complex Intersection

Radha Reddy
Luís Almeida
Pedro Miguel Santos
Harrison Kurunathan
Eduardo Tovar

CISTER-TR-240901

2024

Energy Savings and Emissions Reduction of BEVs at an Isolated Complex Intersection

Radha Reddy, Luís Almeida, Pedro Miguel Santos, Harrison Kurunathan, Eduardo Tovar

CISTER Research Centre

Rua Dr. António Bernardino de Almeida, 431

4200-072 Porto

Portugal

Tel.: +351.22.8340509, Fax: +351.22.8321159

E-mail: reddy@isep.ipp.pt, lda@fe.up.pt, pss@isep.ipp.pt, jhk@isep.ipp.pt, emt@isep.ipp.pt

https://www.cister-labs.pt

Abstract

Improving urban dwellers quality of life requires mitigating traffic congestion, minimizing waiting delays, and reducing fuel wastage and associated toxic air pollutants. Battery-electric vehicles (BEVs) are envisioned as the best option, thanks to zero exhaust emissions and regenerative braking. BEVs can be human-driven or autonomous and will co-exist with internal combustion engine vehicles (ICEVs) for years. BEVs can help at complex intersections where traffic is saturated. However, their benefits can be reduced by poor intersection management (IM) strategies that coordinate mixed traffic configurations inefficiently. This paper studies energy savings and emissions reduction using BEVs mixed with human-driven ICEVs under eight relevant IM approaches. It shows that adding BEVs has impacts on throughput, energy consumption, waiting delays, and tail-pipe emissions that depend on the specific IM approach used. Thus, this study provides the information needed to support an optimal choice of IM approaches considering the emerging trend towards electrical mobility.

© 2024 CISTER Research Center
www.cister-labs.pt

Transportation Research Part D 136 (2024) 104403

Contents lists available at ScienceDirect

Transportation Research Part D

journal homepage: www.elsevier.com/locate/trd

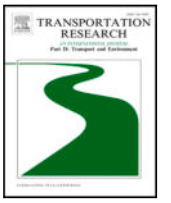

Energy savings and emissions reduction of BEVs at an isolated complex intersection☆

Radha Reddy [a,d,*], Luis Almeida [a,c], Pedro M. Santos [a,b], Harrison Kurunathan [a,b], Eduardo Tovar [a,b]

[a] CISTER Research Center, Rua Alfredo Allen, 535, Porto, 4200-135, Portugal
[b] ISEP - Instituto Superior de Engenharia do Porto, R. Dr. António Bernardino de Almeida 431, Porto, 4200-135, Portugal
[c] FEUP - Faculdade de Engenharia da Universidade do Porto, Porto, 4200-465, Portugal
[d] Department of Computer Science and Engineering, Amrita School of Computing, Amrita Vishwa Vidyapeetham, Coimbatore, TN, 641112, India

ARTICLE INFO

Keywords:
Intersection management
Battery electric vehicles
Internal combustion engine
Human-driver control
Autonomous control
Energy savings
Emissions reduction

ABSTRACT

Improving urban dwellers quality of life requires mitigating traffic congestion, minimizing waiting delays, and reducing fuel wastage and associated toxic air pollutants. Battery-electric vehicles (BEVs) are envisioned as the best option, thanks to zero exhaust emissions and regenerative braking. BEVs can be human-driven or autonomous and will co-exist with internal combustion engine vehicles (ICEVs) for years. BEVs can help at complex intersections where traffic is saturated. However, their benefits can be reduced by poor intersection management (IM) strategies that coordinate mixed traffic configurations inefficiently. This paper studies energy savings and emissions reduction using BEVs mixed with human-driven ICEVs under eight relevant IM approaches. It shows that adding BEVs has impacts on throughput, energy consumption, waiting delays, and tail-pipe emissions that depend on the specific IM approach used. Thus, this study provides the information needed to support an optimal choice of IM approaches considering the emerging trend towards electrical mobility.

1. Introduction

Emissions of particulate matter (PM_x), nitrogen oxides (NO_x) and carbon monoxide (CO) are on the list of UN-designated toxic air pollutants, and the hydrocarbons (HC) and carbon dioxide (CO_2) are also responsible for damaging the environment and human health (UN and WHO, 2016). According to the European Environment Agency, more than 80% of European urban dwellers are exposed to higher concentrations than the recommended annual limit of CO, PM_x, and NO_x, mainly observed at traffic stations and intersections (Grossberndt and Bartonova, 2021). This exposure can cause heart disease and stroke, lung cancer, respiratory diseases, and ultimately death. These complications are expected to worsen in high-income and middle-income countries and continue to rise in low-income countries (WHO, 2022; Koengkan et al., 2022). A few studies from pre-pandemic traffic conditions focused on the excess fuel consumption and associated emissions due to congestion at intersections. For example, Choudhary and Gokhale

☆ This work was partially supported by FCT/MCTES, within the Research Units: CISTER, ISEP/IPP UIDP/UIDB/04234/2020. This work is also a result of [ref. NORTE-01- 0145-FEDER-000073] supported by Norte Portugal Regional Operational Programme (NORTE 2020), under the PORTUGAL 2020 Partnership Agreement, through the European Regional Development Fund (ERDF), and the project Route 25 [ref. TRB/2022/00061 - C645463824-00000063], funded by the EU/Next Generation, within call no. 02/C05-i01/2022 of the Recovery and Resilience Plan (RRP).

* Corresponding author at: CISTER Research Center, Rua Alfredo Allen, 535, Porto, 4200-135, Portugal.
E-mail addresses: reddy@isep.ipp.pt (R. Reddy), lda@fe.up.pt (L. Almeida), pss@isep.ipp.pt (P.M. Santos), jhk@isep.ipp.pt (H. Kurunathan), emt@isep.ipp.pt (E. Tovar).

https://doi.org/10.1016/j.trd.2024.104403
Received 14 November 2023; Received in revised form 31 July 2024; Accepted 31 August 2024
Available online 11 September 2024
1361-9209/© 2024 The Author(s). Published by Elsevier Ltd. This is an open access article under the CC BY-NC-ND license (http://creativecommons.org/licenses/by-nc-nd/4.0/).

Acronyms

BEAVs	battery-electric autonomous vehicles
BEVs	battery-electric vehicles
ICEVs	internal combustion engine vehicles
IIM	intelligent intersection management
ITLC	Intelligent Traffic Light Control
MCA	Max-pressure Control Algorithm
QTLC	Q-learning-based Traffic Light Control
RR	Round-Robin
SIMP	Synchronous Intersection Management Protocol
TTLC	Trivial Traffic Light Control
WTLC	Webster's Traffic Light Control

(2016) observed that intersection congestion in peak hours led to 2–7 times more emissions in Guwahati, India; Bharadwaj et al. (2017) saw that peak hours in intersections caused $\sim$ 51% of more travel delays producing 53% more CO_2 emissions in Mumbai Metropolitan Region; while Gately et al. (2017) observed 113 million gallons of excess fuel consumption in eastern Massachusetts due to congestion at intersections. The research on post-pandemic traffic patterns suggests the need for intelligent and sustainable urban mobility as commuters opt for private vehicles rather than public transport or ride-sharing services (Das et al., 2021). This indicates that traffic congestion conditions are expected to be worse and more diverse than in pre-pandemic conditions. Urban transportation must be intelligent as it highly influences urban dwellers quality of life, impacting travel delays, fuel costs, health conditions, and environmental sustainability. According to the United States Department of Energy,[1] sustainable transportation requires low- and zero-emission energy-efficient transportation, including electric/alternative/bio-fuel vehicles.

To cope with the traffic issues, connected, autonomous and electric vehicles have been introduced (Alkheir et al., 2018; Sadeghi et al., 2020). Among these, battery-electric vehicles (BEVs) emerged following environmental concerns and fuel costs. In this study, we consider BEVs either operated by human drivers (simply BEVs) or autonomous (BEAVs). As a baseline, we will also consider human-driven gasoline internal combustion engine vehicles (ICEVs)[2] Human-driven vehicles (BEVs and ICEVs) and autonomous vehicles (BEAVs) tend to exhibit different driving behaviors (Krauß, 1998; Milanés and Shladover, 2014; Xiao et al., 2017), that may impact traffic and energy consumption efficiency; we model these different behaviors with appropriate car-following models (CFM) that determine the speed of a vehicle in isolation and when approaching other vehicles in front. Furthermore, both BEVs and BEAVs are energy-efficient through regenerative braking and are environmentally friendly due to zero tailpipe emission of toxic air pollutants. Research studies have predicted increased BEV penetration and addressed energy efficiency and emission characteristics. Examples include the life-cycle assessment (LCA) to study the CO_2 emissions and environmental effects (Kawamoto et al., 2019; Lattanzio and Clark, 2020; Verma et al., 2022; Middela et al., 2022); the well-to-wheel-based estimation of energy efficiency and emissions (Faria et al., 2012; Athanasopoulou et al., 2018; Sheng et al., 2021); energy efficient powertrain models (Mamarikas et al., 2022), and the environmental feasibility of using electric vehicle taxis (Singh et al., 2019). The effect on greenhouse gas emissions by introducing BEVs in 29 European Union countries between 2010 and 2020 is also explored (Fuinhas et al., 2021). These works analyzed mixed BEVs and ICEVs scenarios, thus generally considering human drivers. On the other hand, only a few research studies have considered BEAVs. Some examples include energy-efficient cruise driving (Lu et al., 2019), trajectory control (Li et al., 2016), energy optimization (Zhang et al., 2021a), and ride-sharing (Iacobucci et al., 2018).

Beyond vehicles, intersection management (IM) can also impact the sustainability of the transportation system. Studies of mixed ICEVs/BEVs/BEAVs scenarios on the associated energy savings and emissions at isolated complex intersections are not commonly found yet, but there are already some examples (Ahn et al., 2020; Reddy et al., 2020). In this work, we aim to study the sustainability of the transportation system in terms of reducing gasoline/electricity consumption and lowering emissions brought by the introduction of BEVs/BEAVs in scenarios of co-existence with ICEVs at complex intersections. The efficiency of different IM approaches is a second dimension that we include in this study. For this, we consider eight state-of-the-art IM approaches: Round-Robin (RR) (Alekszejenkó and Dobrowiecki, 2019), Trivial Traffic Light Control (TTLC) (Björck and Omstedt, 2018), Max-pressure Control Algorithm (MCA) (Varaiya, 2013), Webster's Traffic Light Control (WTLC) (Webster, 1958), Intelligent Traffic Light Control (ITLC) (Younes and Boukerche, 2014), Q-learning-based Traffic Light Control (QTLC) (Abdulhai et al., 2003), and the Synchronous Intersection Management Protocol (SIMP) for dedicated (SIMP-D) and shared (SIMP-S) left-crossing lanes (Reddy et al., 2023a). These were chosen for being representative of four IM categories, namely conventional (RR and TTLC), intelligent (ITLC and QTLC), adaptive (MCA and WTLC), and reactive (SIMP-D and SIMP-S). In another dimension, the last six IM approaches (ITLC, QTLC, MCA,

[1] https://www.energy.gov/eere/sustainable-transportation

[2] We exclude from the study the existence of autonomous ICEVs, taking as reference legislation such as the EU mandate that all vehicles produced from 2035 onwards must be electric (IEA, 2022), and that the foreseen temporal horizon for the introduction of Level 5 autonomy matches or even exceeds that date (Khan et al., 2022).

WTLC, SIMP-D, and SIMP-S) fall under the intelligent intersection management (IIM) category. Note also that each IM approach has different infrastructure requirements. Thus, this study is also relevant for stakeholders such as urban traffic planners and managers (notably municipalities) that wish to maximize the lifetime of investments in road infrastructure by opting for a solution that ensures efficient intersection operation considering emerging trends in mobility paradigms (e.g., presence of autonomous vehicles and/or V2X communications).

We carried out this study using the SUMO simulator (Lopez et al., 2018). We implemented the IM approaches referred to above in near-saturated traffic conditions with passenger cars, only, and considered mixed ICEVs/BEVs traffic scenarios for varying BEVs/BEAVs penetration ratios. We present results in terms of the intersection throughput, waiting delays, gasoline/electricity consumption, and emission of toxic air pollutants (PM_x, NO_x, CO, CO_2, and HC). The results show that introducing BEAVs significantly decreases the average fuel consumption and pollutant emissions by inducing a smoother, less jerky traffic behavior. Siding with this, the SIMP protocol that also implements a smooth intersection crossing behavior allows attaining the highest throughput, lowest delays and fuel wastage and associated emissions, thus being the best IIM candidate to enable a seamless and sustainable co-existence of BEVs/BEAVs and ICEVs.

Our study uniquely contributes to the existing literature in two key ways. Firstly, we consider the increasing penetration ratios of human-driven and autonomous BEVs mixed with gasoline ICEVs, a scenario that has not been sufficiently explored. Secondly, we estimate the operational efficiency of various types of IM approaches, including conventional, intelligent, adaptive, and reactive. We analyzed performance metrics such as intersection throughput and waiting delays, energy savings, and reduction of toxic tailpipe emissions. This comprehensive approach to studying the interaction between different vehicle types and IM strategies is a novel addition to the field, offering valuable insights for transportation researchers, policymakers, and urban planners.

The rest of the paper is organized as follows: We review the relevant related works in Section 2. Section 3 describes the complex multi-lane signalized intersections. Section 4 describes both fuel consumption models (gasoline and electricity) and emission models (gasoline). Section 5 outlines the state-of-the-art IM protocols used for comparison. In Section 6, the simulation scenario, parameters, and associated values are presented. The performance of the compared IM approaches is presented in Section 7. The limitations of this study are specified in Section 8. Final remarks are drawn in Section 9.

2. Related works

This section reviews the relevant existing works in two aspects: the impact of introducing BEVs/BEAVs mixed with ICEVs and the geographical scope addressing region, city-wide or network of intersections, and isolated intersections.

2.1. Impact of introducing battery-electric vehicles

The impacts of introducing BEVs/BEAVs mixed with ICEVs were studied primarily focusing on energy efficiency and the emission of CO_2. For this purpose, researchers have employed different methodologies, including the well-to-wheel, i.e., from the energy extraction to the consumption in the vehicle (Faria et al., 2012; Athanasopoulou et al., 2018; Sheng et al., 2021), life-cycle assessment (LCA), i.e., from the vehicle production until its end of life plus the distance it traveled (Kawamoto et al., 2019; Bieker, 2021; Middela et al., 2022), powertrain models (Mamarikas et al., 2022), and combinations of these methodologies (García et al., 2023).

With respect to the well-to-wheel methodology, Faria et al. (2012) compared the CO_2 emissions produced by the electricity generation from traditional fuels, the ownership cost, and the impact of BEV driving cycles, i.e., the BEVs performance during various speed conditions with respect to the electricity consumption and CO_2 emissions. Meanwhile, Mamarikas et al. (2022) considered more than 100 driving cycles using powertrain modeling but only studied energy (fuel and electricity) consumption results. On the other hand, Athanasopoulou et al. (2018) compared the estimated and approved CO_2 emissions for ICEVs (gasoline and diesel) and BEVs. A comparative study on energy savings and CO_2 emissions using various fuel-powered and plug-in electric vehicles and BEVs was carried out by Sheng et al. (2021). The studies reported by Liu et al. (2020) and Ramírez-Díaz et al. (2023) focused on medium- and heavy-duty vehicles, while those referred previously focused on passenger car vehicles.

The LCA methodology was used by Kawamoto et al. (2019) for comparing the CO_2 emissions of ICEVs (gasoline and diesel) and BEVs. This work found that BEVs estimated CO_2 emissions are higher than those of ICEVs due to additional CO_2 emissions from battery production. When renewable energy sources were considered, the BEVs CO_2 emissions were lesser than those of ICEVs. In a similar study, Bieker (2021) considered the global implications of BEVs. Watabe and Leaver (2023) also employed LCA but considered both CO_2 emissions and marginal cost to adopt BEVs in Japan fully. Similarly, Koroma et al. (2022) considered the LCA approach studying CO_2 and $PM_{2.5}$ emissions with respect to electricity charging, battery efficiency fade, battery refurbishment, and recycling. Hill et al. (2023) used the LCA methodology and found that the BEVs production initially generates higher CO_2 emissions than ICEVs. Still, over time, it can be reduced up to 60% in European Union traffic conditions and it is projected to reach 80% or more by 2050. Conversely to the previous works that considered passenger cars, Middela et al. (2022) provide an example of using LCA for freight transportation.

A combination of the well-to-wheel and LCA methodologies for different powertrains is used by García et al. (2023) to understand the impact of BEVs in CO_2 emissions against margins set by the European Union. Overall, these well-to-wheel and LCA-based approaches have mainly focused on introducing BEVs and studying energy efficiency and CO_2 emissions. The reported works clarify that introducing BEAVs and associated sustainability analysis (energy efficiency and toxic emissions) is nontrivial.

2.2. Geographical scope

Considering the geographical scope, we reviewed research works that focused on BEVs/BEAVs mixed with ICEVs in a region, a city or network of intersections, and in isolated intersections (Marmaras et al., 2017; He and Wu, 2018; Patella et al., 2019; Kawamoto et al., 2019; Sheng et al., 2021; Ahn et al., 2020; Zhao et al., 2021; Dong et al., 2022; Zhang et al., 2021b).

At the regional level, various studies have estimated the carbon footprint of BEVs in different regions. For example, Kawamoto et al. (2019) considered the United States, the European Union, Japan, China, and Australia, while Bieker (2021) analyzed the European Union, the USA, China, and India. Both works used the LCA method to estimate BEVs CO_2 emissions. Conversely, the well-to-wheel analysis is used by Sheng et al. (2021) to evaluate the CO_2 emissions and energy consumption on the BEV markets of Australia and New Zealand. Hill et al. (2023) presented a study on the European Union's 27 countries. They analyzed the CO_2 emissions of BEVs using LCA and provided policy recommendations. They also assessed the effects of technical and legislative developments on the potential outlook up to 2050. Watabe and Leaver (2023) discussed the adaptation of BEVs in Japan and forecasted their CO_2 emissions for 2050 and 2060. The study aimed at determining whether introducing BEVs will lead to carbon neutrality.

At the city or network of intersections level, Patella et al. (2019) used LCA to simulate the CO_2 emissions of BEVs in Rome, assuming 100% adoption. Meanwhile, Middela et al. (2022) estimated the emissions of freight BEVs in Chennai, India, by measuring onboard emissions and trip characteristics. In another study, Mamarikas et al. (2022) considered the energy consumption of BEVs and ICEVs in urban road networks with various powertrain models. Chen and Rakha (2022) integrated an Eco-Cooperative Adaptive Cruise Control at Intersections controller with a multi-objective dynamic router to save energy and reduce travel delays in the Greater Los Angeles Area. Lastly, Ahn et al. (2023) tested an Eco-Cooperative Automated Control system for BEVs with three different congestion levels (no, mild, and heavy) in a microscopic traffic simulation environment, taking into account energy-efficient routes, vehicle speed evolution, motion, and control.

At the isolated intersection level, Ahn et al. (2020) studied the impact of IM on a roundabout, highway intersection, and a two-way stop considering BEVs/ICEVs energy consumption as they have different consumption patterns. They found that BEVs are energy efficient at high-speed roundabouts and intersections, while ICEVs are more efficient at a two-way stop sign. Differently, Dong et al. (2022) proposed an energy-efficient driving strategy for various types of BEVs and ICEVs considering traffic queues at a signalized intersection. Similarly, Zhang et al. (2021b) presented an eco-driving control strategy for connected BEAVs at intersections with wireless charging, called W-eco-driving, to decrease the total energy consumption and increase traffic efficiency. Meanwhile, Zhao et al. (2021) analyzed the influence of signal timing on the CO_2 emission of BEVs and ICEVs. They use a set of CO_2 incremental emission models depending on stop rate and control delay to achieve this. They also found that the road section speed and the mixed proportion of BEVs directly impact the vehicles delay at intersections.

2.3. Summary

Different studies have employed various methodologies to understand the impact of introducing BEVs and BEAVs at various levels, namely regional, city, or network of intersections and isolated intersections. Such studies mainly focused on energy efficiency and CO_2 emissions. However, the studies on the differentiated impact of human-driven and autonomous BEVs at complex intersections and in saturated traffic conditions are limited. Moreover, studying toxic air pollutants such as PM_x, NO_x, and CO has not been given sufficient attention. Therefore, our work aims at contributing to fill these gaps specifically analyzing the impact of different IM approaches in isolated complex intersections to manage saturated traffic conditions with BEVs and BEAVs mixed with ICEVs. We study different performance metrics, namely the intersection throughput and associated travel delays, fuel/energy efficiency, and emission of toxic air pollutants (PM_x, NO_x, CO, HC, CO_2).

3. Complex signalized intersections

Signalized intersections can be in various shapes and geographic settings and are significant in urban transportation where multiple road paths cross. The complexity of an intersection increases as the number of approach legs to the intersection increases.[3] Each road can have a lane group indicating a set of inflow/outflow road lanes at the intersection entrance. Traffic light control signals manage intersections over time to avoid conflicts between vehicles arriving from different roads. According to the Highway Capacity Manual (HCM) (HCM, 1997) an intersection is already considered complex with four legs and groups of two incoming lanes per leg. Fig. 1 shows the two most common lane group configurations and respective vehicle movements in complex intersections (HCM, 1997). Our study is restricted to these configurations, but we claim that our results are relevant given their popularity.

The configuration in Fig. 1a includes a left lane dedicated to traffic turning left (L) and a right lane shared by traffic going straight (S) and turning right (R). The configuration in Fig. 1b has the left lane shared by L and S traffic.

Fig. 2 presents an overview of the four-way two-lane isolated intersection that we use in our work. Without loss of generality, we consider 90° angled legs and two outflow lanes per leg, which is beyond the already referred two inflow lanes per leg. In the figure, there are eight lane groups, R_i, where odd indexes ($i = 1, 3, 5, 7$) stand for inflow lanes and even indexes ($i = 2, 4, 6, 8$) for outflow lanes. A further index, j, is used to identify the specific lane inside each lane group. Thus R_{ij} stands for lane j in lane group

[3] https://safety.fhwa.dot.gov/intersection/signal/fhwasa13027.pdf

(or road) i. Index j assumes two values, $j = 1$ and $j = 2$, to refer to the side (right) and center-most (left) lanes, respectively. All inflow and outflow lanes are assumed to be equal in length. This intersection model can easily be adapted to specific real-world intersections by changing geographic settings like road length and angle.

This intersection model considers that the intersection is featured with the necessary sensors to support the IM approaches that will be considered further on, including induction loop detectors and cameras placed appropriately at the intersection entrance and exit points and at some distance away from the intersection on inflow lanes (represented with yellow lines). Note that complex sensors like cameras are only needed when vehicles of different crossing directions share a road lane, while simple induction loop detectors are sufficient for the dedicated left-crossing lanes.

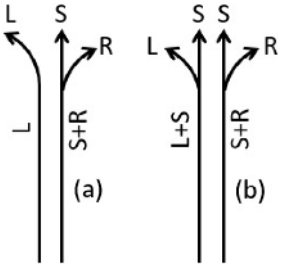

Fig. 1. Two typical lane groups (L, S, and R indicate the left, straight, and right-crossing directions, respectively).

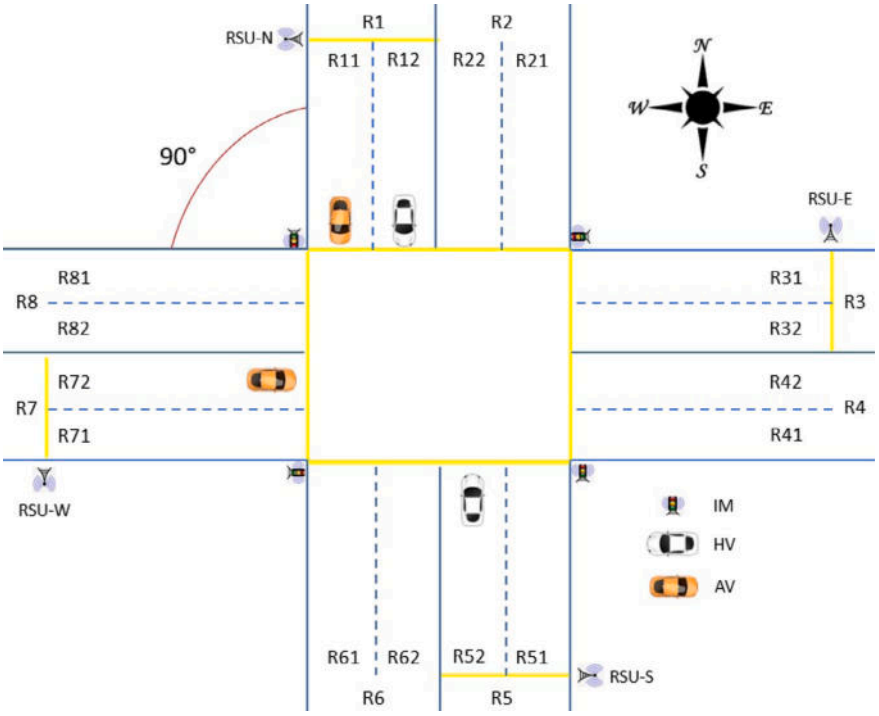

Fig. 2. Four-way two-lane complex intersection.

Our model also considers that all roads are equipped with roadside units (RSU-N, RSU-E, RSU-S, RSU-W) that provide communications to communications-enabled vehicles (e.g., over IEEE 802.11p or 5G). This is in addition to the traffic lights that signal non-communicating vehicles. Though human-driven vehicles can also be communication-enabled without loss of generality, we consider only autonomous vehicles (BEAVs) to have this feature. Therefore, BEAVs can receive information via wireless communications of the traffic light phases and communicate their position and intended crossing direction via the same medium. ICEVs and BEVs are considered non-communicating vehicles and are detected by sensors only. Finally, the RSUs and sensors communicate with the IM unit over wired media (we assume these to be lossless and instantaneous).

Applying the two lane groups shown Fig. 1 to the four-legged intersection in Fig. 2 we obtain the two intersection crossing configurations in Fig. 3, namely dedicated left-crossing (Fig. 3(a)) and shared left-crossing (Fig. 3(b)). This figure also identifies the three types of conflicts (crossing, diverging, and merging) that each configuration exhibits. These conflicts, i.e., locations where

vehicle trajectories diverge, cross, or merge, are points of potential intersection safety incidents, such as crashes (Chandler et al., 2013), and thus need to be explicitly considered by any IM.

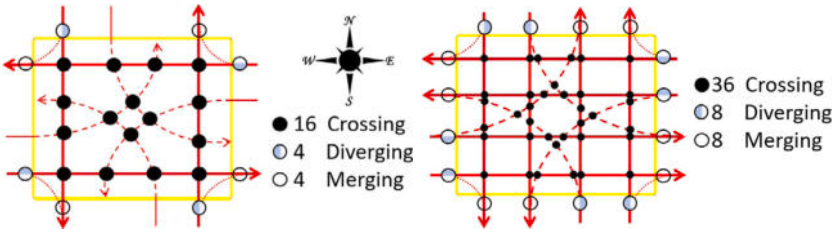

(a) Dedicated left-crossing. (b) Shared left-crossings.

Fig. 3. Two possible configurations of a four-way two-lane intersection.

- Diverging conflicts occur when the single-lane traffic splits to cross different directions at the intersection entrance.
- Crossing conflicts occur when the trajectories of vehicles with different source and destination lanes cross each other inside the intersection.
- The merging conflicts arise when vehicles from different lanes cross the intersection towards the same destination lane at the exit of the intersection.

Each crossing configuration has a different number of crossing, diverging, and merging conflicts. The shared left-crossing configuration (Fig. 3(b)) is more complex, with double diverging and merging conflicts and more than double the crossing conflicts than the dedicated left-crossing configuration (Fig. 3(a)). This work analyzes both configurations in low-speed urban residential areas, particularly subject to a limit of 30 km/h maximum speed.

4. Energy consumption and emissions models

This section presents the fuel (gasoline) consumption model for ICEVs, the associated emissions model, and the electricity consumption model for BEVs and BEAVs that we use in our work.

4.1. Gasoline consumption

The quantification of fuel consumption is based on the Handbook on Emission Factors for Road Transport (HBEFA3.1) (Keller et al., 2010), which is used by the SUMO simulator (Lopez et al., 2018). HBEFA and European Emissions Standard IV state that the emission class PC_G_EU4 characterizes a passenger car with gasoline fuel, i.e., an ICEV. Following HBEFA3.1, the total fuel utilization C in a given vehicle trajectory is defined by Eq. (1), where t_i and t_j indicate the start and end instants in the vehicle path and $Q(t)$ represents the fuel flow.

$$C = \int_{t_i}^{t_j} Q(t)\, dt \tag{1}$$

The fuel flow occurs over a time of t and is estimated with a velocity of $v(t)$ and an acceleration of $a(t)$, i.e., $Q(t) = Q(v(t), a(t))$. The vehicles acceleration (a) and velocity (v) are employed to minimize the impact of error-prone operations for estimating fuel consumption.

4.2. Emissions

The vehicular emissions of a given pollutant p are determined by the corresponding Emissions Factor EF_p. This is a continuous real number that directly depends on the vehicle velocity and acceleration (Lazaro et al., 2009). The HBEFA proposes Eq. (2) to compute the Emissions Factor $EF_p(v, a)$ in time steps considering constant speed v and acceleration a. The e_i parameters and their values are specific to the emission class PC_G_EU4.

$$EF_p(v, a) = \frac{e_0 + e_{va1} va + e_{va2} va^2 + e_1 v + e_2 v^2 + e_3 v^3}{3600} \tag{2}$$

Then, the Emissions Factor EF_p for a given vehicle is obtained by integrating numerically Eq. (2) over all the simulation steps in the vehicle path duration, i.e., from t_i to t_j, as in Eq. (3).

$$EF_p = \sum_{t=t_i}^{t_j} EF_p(v(t), a(t)) \tag{3}$$

The total emissions of different pollutants have different relationships with fuel consumption. For example, emissions of PM_x, NO_x, and CO_2 are directly proportional to fuel consumption. For CO and HC, the emissions estimation also considers the vehicle engine parameters (temperature, speed, and gear), leading to a non-linear relationship and being less accurate than for the other emissions (Lazaro et al., 2009).

4.3. Electricity consumption

The electricity consumption is deduced by observing the loss of the vehicle energy along its path. The energy of a BEV (E_{BEV}) at time instant t is composed of three energy components, namely kinetic (E_k), potential (E_p), and rotational (E_r). These components are determined by parameters such as mass (m), speed over time ($v[t]$), effects of gravity (g) and altitude over time ($h[t]$), and internal rotating moment of inertia (I_i) (Eq. (4)).

$$E_{BEV}[t] = E_k[t] + E_p[t] + E_r[t] = \frac{m}{2} \cdot v^2[t] + m \cdot g \cdot h[t] + \frac{I_i}{2} \cdot v^2[t] \tag{4}$$

Between time steps there is an additional energy loss (ΔE_l) due to resistance components, such as air, rolling, and curve resistance, plus comfort parameters such as air conditioning or heating (Kurczveil et al., 2013).

Therefore, the vehicle energy gain between consecutive time steps t and $t+1$ (ΔE_g) can be estimated using Eq. (5).

$$\Delta E_g[t] = E_{BEV}[t+1] - E_{BEV}[t] - \Delta E_l[t] \tag{5}$$

Note that the energy gain can be negative, e.g., when there is the need to add propulsion, or positive, e.g., when there is regenerative braking. Therefore, the energy variation in the battery (E_{Bat}) should be the variation in the vehicle energy affected by some efficiency coefficient, which is different depending on the process that dominates the gain. For regeneration (i.e., when $\Delta E_g[t] > 0$), the efficiency coefficient is η_r. For propulsion (i.e., when $\Delta E_g[t] < 0$), the efficiency coefficient is η_p.

$$E_{Bat}[t+1] = \begin{cases} E_{Bat}[t] + \Delta E_g[t] \cdot \eta_r & (\Delta E_g[t] > 0) \\ E_{Bat}[t] + \Delta E_g[t] \cdot \eta_p^{-1} & (\Delta E_g[t] < 0) \end{cases} \tag{6}$$

5. Intersection management approaches

As mentioned earlier, this paper uses eight IM approaches that cover different categories and which are either commonly found or proposed by research. Namely, RR and TTLC are conventional, MCA and WTLC are adaptive, ITLC and QTLC are intelligent, and SIMP-D and SIMP-S are reactive. These IM approaches are briefly presented next. Their main characteristics are summarized at the end of this section in Table 1.

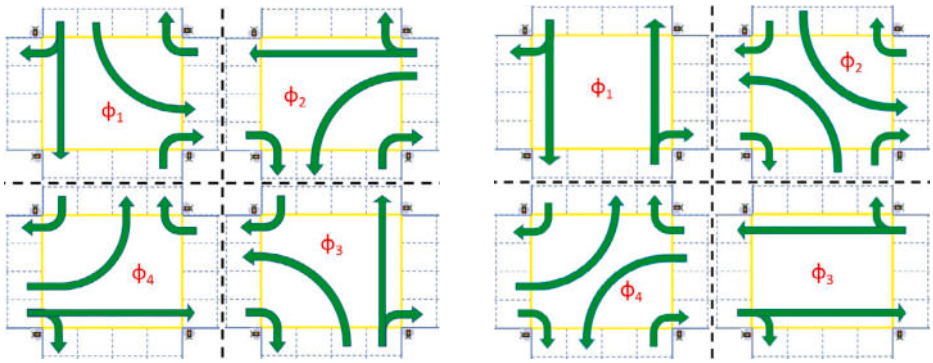

(a) RR and WTLC control phases. (b) MCA, TTLC, ITLC, QTLC control phases.

Fig. 4. Traffic control phases associated to the various IM approaches.

5.1. Round-Robin - RR

RR IM is also called the uniform signal controller due to the uniform green time allocation to all road lanes. RR IM is the conventional IM strategy that periodically alters green-yellow-red phases in a pre-determined circular fashion (Alekszejenkó and Dobrowiecki, 2019). This IM strategy allows vehicles from one lane at a time in a clockwise direction. For instance, when we take a four-way two-lane dedicated left-crossing lane intersection (Fig. 3(a)), every green phase of 30 s is followed by a 4 s yellow phase, and the inflow from the other road lanes will be blocked. The TLC control phases of RR IM are shown in Fig. 4(a). Note that we have tested various green phase times (5 s, 15 s, 30 s, and above) and found that 30 s of green time exhibits the best performance.

5.2. Trivial Traffic Light Control - TTLC

TTLC follows the RR interns as a pre-configured IM strategy that operates periodically (Björck and Omstedt, 2018). In contrast to RR, TTLC allows vehicles from opposite directions, as shown in Fig. 4(b). For instance, when we take a four-way two-lane dedicated left-crossing intersection, the shared right-most lane gets a greater green time of the 30 s than the center-most lane, which equals a half 15 s and a 4 s of yellow time while all other inflow lanes are blocked with red phases.

5.3. Intelligent Traffic Light Control - ITLC

ITLC utilizes real-time traffic characteristics such as queue length, vehicle speed, and acceleration to determine traffic light phases, order, and execution length (Younes and Boukerche, 2014). Using these real-time characteristics, ITLC can improve traffic fluidity and reduce waiting time. For instance, the opposite road lanes with a longer queue length will get the higher priority, and a maximum green time of 60 s is allocated, followed by a 4 s yellow time. The other conflicting inflows to the intersection will be blocked. For shorter queue length, a minimum green time of 5 s followed by 4 s yellow time is allocated. The functioning of ITLC over a four-way two-lane dedicated left-crossing intersection is shown in Fig. 4(b).

5.4. Q-learning-based Traffic Light Control - QTLC

QTLC strategy is designed based on multi-agent systems for reducing vehicle delays (Abdulhai et al., 2003). Akin to the previous IM strategy, QTLC also uses queue length and elapsed phase time for decision-making, and this decision can either continue with the current phase or switch to another phase. Unlike the other IM strategies, this adaptive behavior results in the reduction of vehicle delays. QTLC follows a fixed cycle with a minimum duration of the 20 s and a maximum duration of the 60 s. These cycles also follow an arbitrary limit of 10 s at the beginning and 10 s at the end, in which a 4 s yellow phase follows each green phase. Fig. 4(b) shows the control phases of QTLC.

5.5. Max-pressure Control Algorithm - MCA

MCA measures adjacent lanes instantaneous traffic flow (number of vehicles) movement and then assigns corresponding weights for turn-based movements (Varaiya, 2013). By this, MCA can eventually increase the intersection throughput by bringing stability to the queue pressure in an acyclic manner with dynamic phase lengths. We have tested MCAs various green time (5 s, 15 s, and 30 s) and TLC phases (Fig. 4(a) and 4(b)) configurations. The MCA control phases shown in Fig. 4(b) with the 30 s of green time followed by a 4 s yellow time show the best results.

5.6. Webster's Traffic Light Control - WTLC

WTLC follows a cycle-based traffic signal control for a fixed minimum and maximum allocated time and employs traffic flow data for traffic signal optimization (Webster, 1958). This method collects the traffic flow data for a specified time interval. Then Webster's method calculates the cycle time and green phase duration for that time interval. The adaptive form of WTLC utilizes the most recent time interval to collect data and then assumes that the traffic demand will be the same for the upcoming time interval. In WTLC, the time interval selection is crucial as it can result in various trade-offs. Smaller values can result in frequent adaptations to changing traffic demands, and larger values adapt less frequently. This paper utilizes both minimum (40 s) and maximum (180 s) TLC cycle lengths with a time interval of 450 s, and higher interval times lead to lower performance due to saturated traffic conditions. The WTLC control phases are shown in Fig. 4(a), the same as RR.

5.7. Synchronous Intersection Management Protocol - SIMP

SIMP is an IIM protocol that provides traffic fluidity at complex intersections (Reddy et al., 2023a). SIMP works over two distinctive left-lane configurations employing the intelligent intersection management architecture (IIMA shown in Fig. 2), namely the dedicated left-crossing (SIMP-D) and shared left-crossing (SIMP-S) as presented in Fig. 3(a) and 3(b). SIMP's synchronous nature iterates the following steps cyclically: firstly, finding vehicles at the intersection entrance; deducing the intended crossing directions by utilizing the available sensors; computing vehicles safe crossing using a Conflicting Directions Matrix (CDM); triggering their access to the intersection via traffic lights or wireless messages. This process waits for vehicles within the intersection until the exit. The process is repeated once all vehicles in the intersection have exited it within the short cycle length, leading to the reactive nature. The CDM allows SIMP to track all conflicting directions (presented in Fig. 3(a) and 3(b)) simultaneously at every control cycle, which checks all inflow road lanes.

Table 1
Main properties of the IM approaches under comparison.

IM	Road Infrastructure	Left lane	TLC decision	Green time (s) (S/R & L)	Objective
RR	N	D	F	30 & 30	Manage
TTLC	N	D	F	30 & 15	Manage
ITLC	Y	D	I	[5, 60] & 15	Fluidity & Delays
QTLC	Y	D	I	[20, 60] & 15	Delays
MCA	Y	D	A	30+ & 30+	Traffic stability
WTLC	Y	D	A	[6, 41] & [6, 41]	Optimum signal time
SIMP	Y	D/S	R	2.5 & 3	Fluidity

Notes. Y-yes, N-no, D-dedicated, S-shared, F-fixed, I-intelligent, A-adaptive, and R-reactive.

5.8. Summary of IM approaches properties

Table 1 summarizes the main properties of the IM approaches considered. Among them, ITLC, QTLC, MCA, WTLC, and SIMP require road infrastructure, while the RR and TTLC approaches work on roads without infrastructure. Regarding left lane configurations, SIMP provides both dedicated and shared left lanes. Although all other protocols could also support the shared left lane configuration, we omitted it from this study for consistency with their proposals that considered dedicated left lanes only.

As we referred to before, these IM approaches can be classified into four cases according to their decision-making process, namely conventional, intelligent, adaptive, and reactive. RR and TTLC are the conventional approaches used in this work, which present a fixed cycle independent of the traffic patterns (for this reason, we refer to them here as *fixed*). ITLC and QTLC present an intelligent behavior that changes the cycle according to the current traffic intensity in the different lanes. MCA and WTLC present an adaptive behavior in traffic signal timing reflected in the traffic lights control cycle length (minimum, maximum, or both) based on the traffic intensities on different road lanes. Differently, SIMP takes a reactive approach that responds to the presence of individual vehicles at the entrance of the intersection.

In the table, under the green time column, the S/R lane indicates the rightmost lane that shares the straight-/right-crossing vehicles, and the L lane indicates the left-crossing lane that can be either dedicated to left-crossing or shared between straight-/left-crossing vehicles. MCA is acyclic but has a minimum green time, so we indicated it with + . The values indicated in the table and used in this paper are those proposed by the respective references.

The main objectives driving the development of the IM approaches are shown in the last column. While RR and TTLC simply aim at managing the traffic to avoid collisions, SIMP also aims at increasing the fluidity of the traffic, and QTLC at reducing average delays. On the other hand, ITLC aims to achieve both fluidity and delay reduction, MCA aims to minimize the traffic intensity in the road network, and WTLC aims to optimize traffic signal timing.

6. Simulation setup

In our simulation study, we designed and simulated two mixed traffic scenarios to analyze energy savings and emissions volume when crossing one complex intersection controlled by a specific intersection management approach. The mixed traffic scenarios considered an increasing penetration of human-driving BEVs and autonomous BEAVs together with human-driven ICEVs.

In the first scenario, ICEVs and BEVs follow the Krauss car-following model (Krauß, 1998) that represents typical human driving behavior. This scenario showcases the increased energy efficiency and decreased emission of air pollutants obtained from employing human-driven BEVs. We observe these effects under the various IM approaches applied to the intersection to see which approach can benefit the most when introducing human-driven BEVs, and which performs more sustainably in absolute terms.

In the second scenario, ICEVs follow the same Krauss CFM simulating human-driven vehicles, while BEVs become BEAVs equipped with autonomous control (ACC CFM (Milanés and Shladover, 2014; Xiao et al., 2017)). This scenario studies the impact of introducing BEAVs in the overall fuel consumption and emissions of the ICEVs. As in the previous case, we apply the referred eight IM approaches to the intersection to understand which is impacted the most when adding BEAVs.

The previously described IM approaches are deployed on an isolated four-way two-lane intersection using the SUMO framework v1.12.0 under identical geographic settings. The simulator runs on an Intel Core-i5 8th-generation CPU with 4 cores @1.60 GHz, 8 GB RAM, and a 64-bit Windows 11 OS.

The simulated time is one hour (3600 s). The inflow and outflow road lanes connecting to the intersection are 500 m long and flat. We also consider a maximum speed of 30 km/h, which represents typical low-speed urban settings. With these settings, the simple road system we consider, with a single complex flat intersection, is a key component to building general urban road systems. According to the results shared in Reddy et al. (2023a), most of the IM approaches that we consider saturate at 0.2 veh/s (i.e., 12 vehicles per minute) in a similar setting, so we choose the same traffic arrival rate. To apply this arrival rate, at every second, we sample from a uniform distribution in the range $[0, 1]$ and inject a vehicle if the sample is inferior to the selected arrival rate. At this arrival rate, in 1 h, we inject an average of 720 vehicles in the road system. Assignment of intended trajectory to vehicles also uses samples from a uniform distribution. Vehicles are distributed with equal probability for left (33%), straight (33%), and right

(33%) crossings in all experiments[4] (Reddy et al., 2023a,b). This means that we are injecting, on average, 240 vehicles per crossing direction in each 1 h experiment. Vehicles assigned to the left are injected in the leftmost lane, and those assigned to the straight and right are injected in the rightmost lane. Finally, each experiment is run five times with different random seeds but with the same set of parameters. Hence, each data point is the average of five runs, involving a total of 3600 vehicles on average, 1200 to each crossing direction.

The acceleration (2.6 m/s^2), deceleration (−4.5 m/s^2), and emergency deceleration (−9 m/s^2) values are adopted from the SUMO default values.[5] Other simulation parameters like the minimum time headway between consecutive cars (1 s) and the driving imperfection (0.5 for ICEVs and BEVs and 0.0 for BEAVs) are applied to the CFMs described earlier. Using these simulation parameters values, particularly for the Krauss CFM running at a free-flow maximum speed of 30 km/h, i.e., 8.33 m/s, results in a jerky speed pattern presented in Fig. 5(a). When using the ACC CFM in autonomous vehicles, the resulting speed pattern is presented in Fig. 5(b).

Table 2 summarizes the main simulation parameters and their assigned values concerning ICEVs, BEVs, and BEAVs. Table 3 presents parameters that are specific to BEVs/BEAVs, representing an average electric passenger car (Helmers and Marx, 2012).

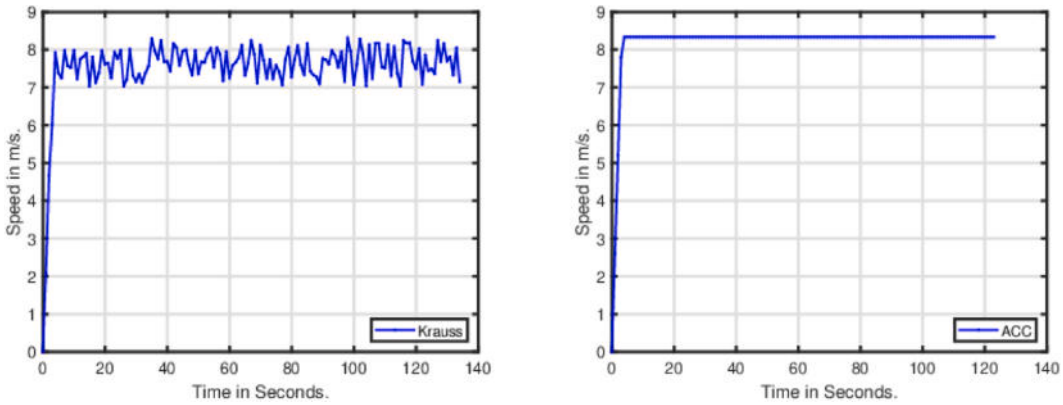

(a) Jerky driving behavior using Krauss CFM (ICEVs/BEVs) (b) Smooth driving behavior using ACC CFM (BEAVs)

Fig. 5. Driving behaviors of ICEVs/BEVs and BEAVs.

Table 2
Simulation parameters and assigned values.

Parameters	Values
Probability of vehicle insertion	Uniform distribution [0 1]
Vehicle type	Human-driven (Krauss) and Autonomous (ACC)
Vehicle length	5 m
Safety distance (target)	5 m
Fuel type	Gasoline (ICEVs) and Electricity (BEVs/BEAVs)
Fuel consumption model	HBEFA3.1 (ICEVs) and Battery Electric (BEVs/BEAVs)
Target speed	30 km/h, i.e., 8.33333 m/s
Acceleration	2.6 m/s^2
Deceleration	−4.5 m/s^2
Emergency deceleration	−9 m/s^2
Minimum time headway	1 s
Drivers imperfection	0.5 (Human-driven) 0.0 (Autonomous)

[4] In our previous studies, we also employed the Poisson distribution to generate the traffic and tested both continuous and interrupted traffic flow conditions

[5] https://sumo.dlr.de/docs/Vehicle_Type_Parameter_Defaults.html

Table 3
Parameters specific for BEVs/BEAVs.

Parameters	Values
Max. battery capacity	64 kWh
Max. power	150 kW
Constant power intake	100 W
Internal moment of inertia	0.01 Kg m^2
Air drag coefficient	0.35
Radial drag coefficient	0.5
Roll drag coefficient	0.01
Propulsion efficiency	0.98
Recuperation efficiency	0.96
Stopping threshold	0.1 km/h

7. Results and discussion

We now discuss intersection management performance metrics (intersection throughput and waiting delays) as we increase the penetration of battery-electric vehicles from 10% to 90% (both for BEVs and BEAVs). We then carried out a similar exercise but focused on energy savings (gasoline and electricity) and emission of air pollutants (PM_x, NO_x, CO, HC, and CO_2). The sustainability of the various IMs is tightly linked to the intersection performance; hence, analyzing throughput and average waiting times is relevant before discussing fuel consumption and emissions.

7.1. Intersection performance metrics

*7.1.1. Intersection throughput (*veh/h*)*

Fig. 6 shows the intersection throughput results for various penetration ratios of BEVs (Fig. 6(a)) and BEAVs (Fig. 6(b)). We consider the intersection throughput as the number of vehicles an IM approach serves in an hour (3600 s).

The BEV scenario results (Fig. 6(a)) show clearly that throughput is not affected by the nature of the vehicles propulsion, which is expected since BEVs are human-driven such as ICEVs, thus their motion behavior is similar. On the other hand, the results for BEAVs (Fig. 6(b)) show a visible increase in throughput for all IMs, particularly the ones exhibiting lower values. This difference emerges from the speed feedback control of BEAVs that increases the average speed and reducing the headway (respecting safety distance) to the vehicle ahead when compared to human-driven vehicles, leading to more vehicles crossing the intersection per unit of time than when more human-driven vehicles (ICEVs) are used.

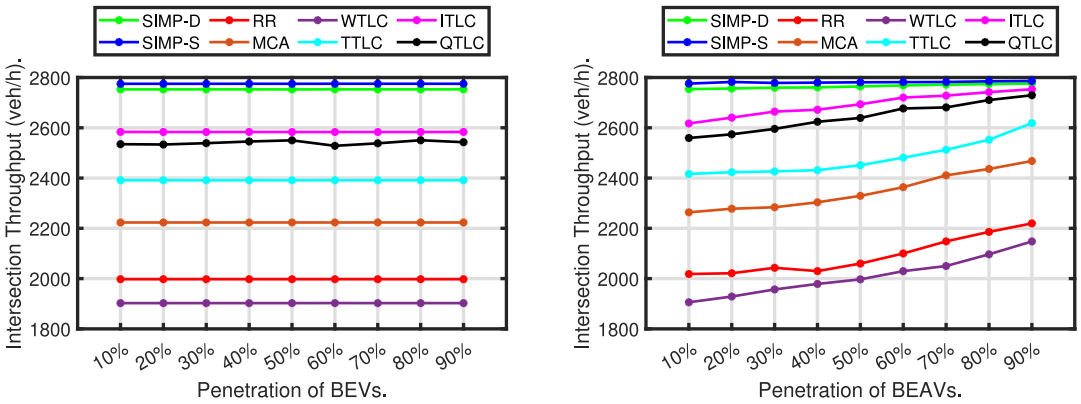

(a) Throughput against penetration of BEVs.

(b) Throughput against penetration of BEAVs.

Fig. 6. Intersection throughput (veh/h) of different IM approaches for various BEVs and BEAVs penetration ratios.

Concerning the different IMs, we observe that the highest throughput is achieved with both SIMP configurations, with a slight advantage for SIMP-S over SIMP-D, while WTLC shows the lowest throughput. When the traffic is ICEVs (or BEVs)-dominated,

WTLC serves approximately 900 vehicles less, in 1 h, than any of the SIMP approaches, i.e., a reduction of approximately 32% in throughput. This difference is reduced to about 600 vehicles, i.e., approximately 21%, in a BEAVs-dominated scenario.

Overall, taking the throughput of SIMP-S as reference (2775 veh/h - 100%), the ratios achieved by the other IMs in an ICEVs (or BEVs)-dominated scenario are the following: 99.2% for SIMP-D, 93.09% for ITLC, 91.54% for QTLC, 86.17% for TTLC, 80.11% for MCA, 71.98% for RR and 68.55% for WTLC. When moving to a BEAVs-dominated scenario, i.e., with a 90% penetration of BEAVs, all IM approaches experience relative increases in throughput as follows: SIMP-D increases 0.8134%, ITLC increases 5.2%, QTLC increases 6.64%, TTLC increases 8.36%, MCA increases 9.02%, RR increases 9.98% and WTLC increases 12.7%. These values confirm that the IM approaches that benefit the most from introducing BEAVs are those with lower throughput, particularly for penetrations above 50%.

In the BEAVs-dominated scenario, ITLC and QTLC have practically the same throughput as the SIMP approaches, while TTLC achieves 89.14% of the maximum and MCA achieves 84.44%. Despite exhibiting the strongest relative increase, RR and WTLC continue to lag behind, achieving just 75.21% and 72.27% of the throughput of SIMP-S, respectively.

SIMP's throughput performance is due to the very short control cycle time that synchronizes conflict-free vehicle movements, leading to a more regular (smoother) service that results in serving more vehicles per time unit. We can also observe that there is no significant throughput improvement with SIMP approaches (i.e., from 2775 to 2786, 0.22% only) when going from a human-driven (BEVs)-dominated scenario to a scenario dominated by autonomous vehicles (BEAVs). This seems to indicate that SIMP's performance in this dimension is close to optimal.

On the other hand, conventional IM approaches (RR and TTLC) block the road lanes that are not being served for longer periods following their control cycle times, hindering their performance and thus serving fewer vehicles. Differently, ITLC and QTLC adapt their control cycles using traffic characteristics (queue lengths, vehicle speed, and acceleration) and improve the throughput results. MCA and WTLC also adapt the control cycle, but the decisions are inefficient in tackling saturated traffic conditions.

7.1.2. Average waiting time (s)

Due to congestion and traffic signal configurations, vehicles may have to wait to access the intersection, particularly during the yellow and red phases. Apparently, intersection management approaches with longer control cycle times impose longer waiting times, while shorter cycles impose shorter waiting delays. We measure the waiting time of a vehicle as the interval of time from the first moment its speed goes below a given threshold (currently 5 km/h, meaning it arrives at a queue) until it enters the intersection. Fig. 7 displays the average waiting time (s) of vehicles that completed their journey in 1 h of simulated time. As expected, these results are strongly correlated with the throughput results. Naturally, higher throughput means lower average waiting time and vice-versa.

Therefore, the waiting times in the BEVs scenario shown in Fig. 7(a) exhibit similar behavior to the corresponding throughput results in Fig. 6(a), namely independence with respect to the BEVs penetration ratio arising from the fact that both ICEVs and BEVs follow the same human driving behavior. Concerning the actual values, we observe very low values for the SIMP protocols, namely 5 s for SIMP-S and 7 s for SIMP-D, because this management approach favors a continued flow of vehicles, reducing stop-and-go effects. ITLC and QTLC exhibit the next lower values, around 100 s, even though they were designed to reduce the waiting time. Conventional approaches TTLC and RR, together with MCA, exhibit waiting times of around 200 s. The worst IM is WTLC, with an average waiting time of approximately 250 s. Again, these poor performances arise from the fixed nature of the control cycles in the conventional approaches or from an inadequate adaptive mechanism in the adaptive MCA and WTLC approaches, which fail to capture the time-invariant stochastic properties of the injected traffic, either adapting too frequently or too slowly.

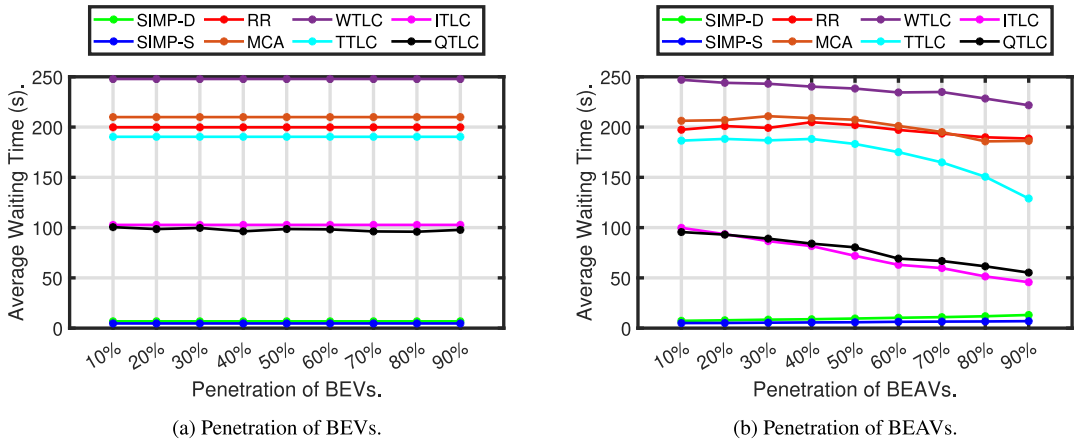

(a) Penetration of BEVs.

(b) Penetration of BEAVs.

Fig. 7. Average waiting time (s) imposed by different IM approaches for various BEVs and BEAVs penetration ratios.

The BEAVs scenario in Fig. 7(b) shows a reducing trend on the waiting times of the different IM approaches when increasing BEAVs penetration. This is consistent with the throughput case. However, the impacts on different IM approaches are now more

variable than in the throughput case. The exception are the SIMP protocols that exhibit now a slight waiting time increase for increasing BEAVs, with SIMP-S adding an extra 1.9 s and SIMP-D 5.8 s in a BEAVs-dominated situation (90% penetration). This behavior seems to emerge from the increased average speed of BEAVs, which makes them approach the intersection faster, leading to slightly more traffic accumulation and potentially more stop-and-go situations.

For the remaining IM approaches, going from 10% to 90% BEAVs penetration causes a waiting time variation of −54.04 s (−54.185%) for ITLC, −40.36 s (−42.224%) for QTLC, −57.54 s (−30.856%) for TTLC, −8.75 s (−4.436%) for RR, −19.96 s (−9.68%) for MCA and −25.3 s (−10.244%) for WTLC. Interestingly, RR and MCA show very low sensitivity to the penetration of BEAVs, while ITLC, QTLC and TTLC exhibit significant reductions, being positively affected by the introduction of autonomous vehicles. This emerges from the slightly higher average speed of the BEAVs that are then served faster in the green phases of the respective IM approaches.

7.2. Energy savings

Fig. 8 shows the average gasoline consumption (ml) per ICEV for the whole path in both scenarios, penetration of BEVs and BEAVs. The results indicate a correlation with waiting time, where a longer waiting time leads to higher fuel consumption. This is due to the additional accelerations of start-stop maneuvers while queuing and to the engine idling while stopped.

Concerning the specific case of introducing BEVs (Fig. 8(a)), we can see again that there is nearly no impact, given that all vehicles, BEVs and ICEVs, have the same driving pattern. However, in this case we observe a slight reduction in the ICEVs consumption when the BEVs penetration goes beyond 60% in almost all IM approaches (except for the SIMP protocols that remain always constant). However, the explanation of this small artifact requires further investigation. But the most relevant result in this case is the large difference in fuel consumption when comparing the different IMs. The smoother behavior of the SIMP protocols compensates in low consumption, reaching approximately 100 ml. QTLC and ITLC, the next IMs in fuel consumption, already exhibit approximately twice that of the SIMP approaches, i.e., around 200 ml. Then the conventional and adaptive approaches vary between 300 ml and 400 ml, i.e., three and four times the consumption with the SIMP approaches.

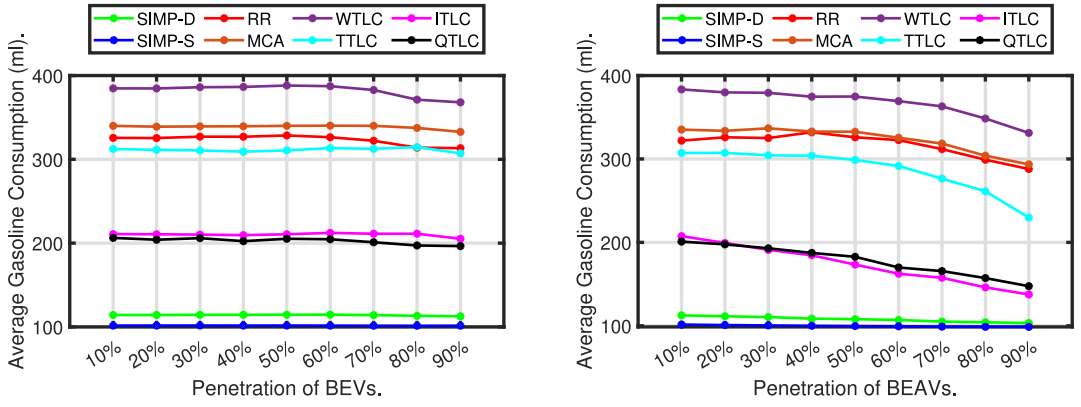

(a) Penetration of BEVs. (b) Penetration of BEAVs.

Fig. 8. ICEVs average gasoline consumption (ml) when introducing BEVs and BEAVs under different IM approaches.

When introducing BEAVs, the results show a pattern very similar to that of the waiting times of the corresponding scenario. All IMs but the SIMP protocols show a significant reduction in consumption, which reveals itself as soon as BEAVs are introduced (ITLC and QTLC cases) or for penetrations above 50% (all other cases). The reductions achieved are the following: −53.4 ml (−26.58%) for QTLC, −69.9 ml (−33.69%) for ITLC, −77.3 ml (−25.1%) for TTLC, −34.0 ml (−12.4%) for RR, −41.6 ml (−13.6%) for MCA, and −52.1 ml (−25.1%) for WTLC. These values show that the impact of introducing BEAVs can be significant on the fuel consumption of the ICEVs, particularly under ITLC, QTLC and TTLC. We attribute this effect to a smoothing of the ICEV driving behavior given that, as BEAVs penetration increases, human-driven ICEVs will be more likely to follow smoother-driving vehicles.

The average electricity consumption (Wh) results of BEVs and BEAVs penetration scenarios are presented in Fig. 9. Note that the two types of electric vehicles use different car-following models, namely BEVs use Krauss CFM and BEAVs use ACC CFM. It is also worth mentioning that both types of these vehicles employ regenerative braking, meaning that the slowing down and stopping actions involved in queuing and synchronizing at the intersection entrance recover part of the energy spent accelerating and traveling, improving energy efficiency compared to ICEVs.

Fig. 9(a) shows the average electricity consumption of BEVs as their penetration increases. As expected, there is practically no dependence on the penetration ratio, given the similar driving behavior of BEVs and ICEVs. Moreover, the relative performance of the different IMs is also similar to the previous cases, with the SIMP protocols showing the lowest energy consumption, followed by ITLC and QTLC, and then the group of conventional and adaptive IMs. However, there is a significant difference with respect to the previous results on fuel consumption, i.e., the variations in electricity consumption across the IMs are now smaller than in

the corresponding scenario on fuel consumption. From the results, SIMP-S and SIMP-D show an average electricity consumption of approximately 94.5 Wh and 95 Wh, followed by ITLC and QTLC that consume around 98 Wh, i.e., an increase of just 3.7% to SIMP-S. Then, the other group (TTLC, RR, MCA, and WTLC) consumes around 102 Wh, thus an increase of 7.9% to SIMP-S. These small differences seem to be related to the higher efficiency of BEVs with respect to ICEVs, including their regenerative braking capability.

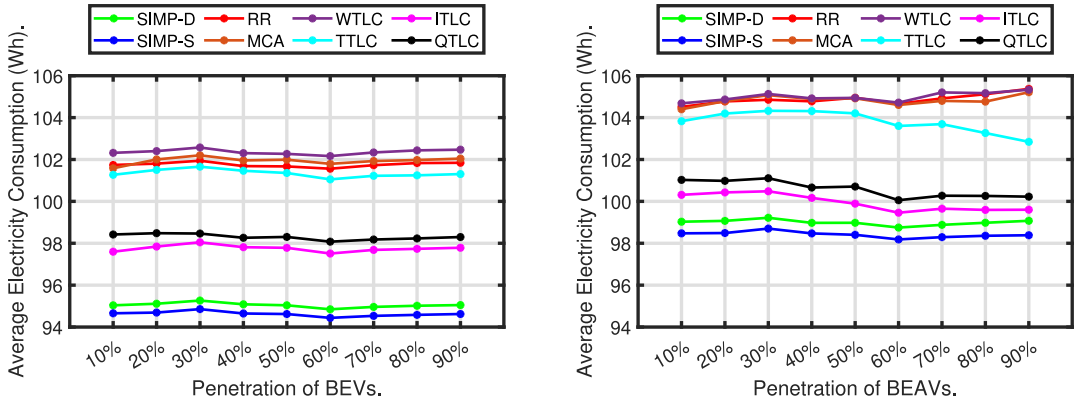

(a) Penetration of BEVs.

(b) Penetration of BEAVs.

Fig. 9. Average electricity consumption (Wh) for BEVs and BEAVs when increasing their penetration under various IM approaches.

Fig. 9(b) shows the BEAVs average electricity consumption with growing penetration ratios. An immediate observation is that, compared to BEVs, BEAVs electricity consumption is slightly higher, caused by the slightly higher average speed (consistent with the higher throughput seen in Fig. 6(b)). For example, the SIMP protocols exhibit an increase of approximately 3.8 Wh, the largest increase, then ITLC and QTLC show an average increase of 2.2 Wh and 2.3 Wh, respectively, with the smallest increase, and finally, the remaining IMs show increases between 2.5 Wh for TTLC and 3.12 Wh for RR.

One result of this differentiated increase is that both reactive and intelligent IM approaches (SIMP, ITLC and QTLC) exhibit now closer electricity consumption, between 98.5 Wh for SIMP-S and 101 Wh for QTLC, when ICEVs dominate (10% BEAVs penetration), and even less, 98.5 Wh to 100 Wh for the same IMs when BEAVs dominate (90% penetration).

Another observation is that the impact of growing BEAVs penetration is now marginal. The reactive IMs (SIMP) remain fairly constant for all penetration ratios. On the other hand, both intelligent approaches (ITLC and QTLC) and the conventional TTLC show a slight reduction of around −1 Wh (−1%) that becomes visible after 50% penetration. Curiously, the IMs of the worse performing group (RR, MCA and WTLC) show a slight increase of around +1 Wh (+0.96%). These behaviors are somewhat intriguing and seem to emerge from two opposite effects related to the interference ICEVs may cause to BEAVs. When a BEAV follows an ICEV, it will try to follow the ICEV's behavior. On one hand, this will reduce the average speed of the BEAV, leading to lower consumption. However, it will also make the BEAV exert more accelerations to follow the jerky ICEV speed profile, which leads to higher consumption. Whether one effect dominates the other depends on specific micro traffic patterns that emerge from the traffic control and the actual speed profiles and further research is required at such a micro level for a better understanding. Nevertheless, our study shows that variations in the electricity consumption of BEAVs as a function of their penetration ratio are not significant.

7.3. Emissions reduction

This section presents the average tail-pipe emissions of ICEVs when increasing the penetration ratios of BEVs and BEAVs. We focus on the emissions of PM_x, NO_x, CO_2, CO and HC. As we reported in Section 4, the models for PM_x, NO_x, CO_2 are directly proportional to the fuel consumption (Fig. 8). This is confirmed in Figs. 10, 11 and 12 for those three types of emissions, respectively. Since these plots are all displaying the same pattern, we simply present the first one here, for PM_x, while the following ones are included in an Annex. We decided to keep the similar figures in an Annex because they have specific information on the actual values, despite the similar pattern. On the other hand, the model for CO and HC is more complex, including specific engine parameters (Section 4). Nevertheless, the results still show a very similar pattern (Fig. 13 for CO and Fig. 14 for HC), just with differences in the ratios between the values of different IMs. For this reason, we also relegate these figures to Annex.

There are two major observations we can make when observing these figures. The first one concerns the relative performance of the different IMs when introducing BEVs. This scenario does not depend on the penetration ratio of BEVs, with ICEVs showing steady emissions levels. The lowest emissions result from the use of the SIMP protocols. Taking these as a reference, with ITLC and QTLC ICEVs exhibit between 1.7 and 2.2 times the emissions of PM_x, NO_x, and CO_2 and between 3.4 and 3.9 times the emissions of CO and HC. With the other IMs (TTLC, RR, MCA and WTLC) ICEVs exhibit between 3.1 and 5.5 times the emissions of PM_x, NO_x and CO_2 than with the SIMP protocols and about 6 and 8.6 times the emissions of CO and HC. These are significant differences.

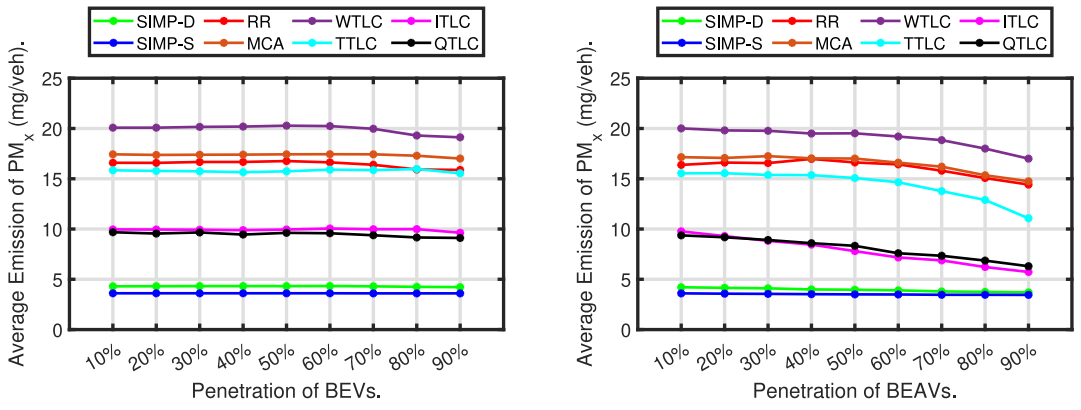

(a) Penetration of BEVs.

(b) Penetration of BEAVs.

Fig. 10. Average emission of PM_x (mg) per ICEV under several IM approaches and with growing BEVs and BEAVs penetrations.

The second observation is that the growing penetration of BEAVs causes ICEVs to produce lower emissions under all IMs except with the SIMP protocols, which causes ICEVs to produce steady emissions independently of the BEAVs penetration ratio. Therefore, the relative performance of all IMs with respect to SIMP protocols improves in BEAVs-dominated (90% penetration) scenarios. The reason is the lower fuel consumption resulting from ICEVs following BEAVs, as explained in Section 7.2. In particular, again taking the emissions under the SIMP protocols as a reference, with ITLC and QTLC ICEVs exhibit between 1.4 and 1.8 times the emissions of PM_x, NO_x, and CO_2 and between 2 and 2.4 times the emissions of CO and HC. With the other IMs (TTLC, RR, MCA, and WTLC), ICEVs exhibit between 2.3 and 4.9 times the emissions of PM_x, NO_x, and CO_2 than with the SIMP protocols and between 4.3 and 7.7 times the emissions of CO and HC.

8. Limitations

This study focused on the energy efficiency (gasoline and electricity), emissions reductions (PM_x, NO_x, CO_2, CO, and HC), intersection throughput, and waiting delays when HVs (ICEVs and BEVs) and AVs (BEAVs) cross a flat complex intersection up to of 30 km/h maximum speed. These results cannot be extrapolated to roads with inclination and/or for higher speeds. The traffic generation process did not account for different ratios of vehicles tending to each possible direction (left, straight, right), which can be expected in many real-world intersections. While we consider the layout of the used intersection representative, the results cannot be extrapolated to other configurations. Our analysis focuses on two car-following models (Krauss and ACC); however, manufacturers may implement different control algorithms, notably for platooning, and drivers may demonstrate varying driving styles (e.g., defensive or aggressive), which are not accounted for in this study.

9. Conclusions

This paper presents a novel sustainability analysis examining the penetration of battery-electric vehicles, both human-driven - BEVs - and autonomous - BEAVs - in a baseline of vehicles with gasoline internal combustion engines - ICEVs. The analysis is carried out in the scope of an isolated complex intersection common in low-speed residential areas, considering a 30 km/h maximum speed. Such an intersection is a central element in building urban road systems, thus this study is relevant for urban planners to help in the choice of intersection management approaches - IMs - with awareness to the impact of BEVs and BEAVs.

Our research compares, using the SUMO simulator, the performance of eight relevant IM approaches (reactive: SIMP-D and SIMP-S; intelligent: ITLC and QTLC; conventional: RR and TTLC; and adaptive: MCA and WTLC) when increasing the penetration of BEVs and BEAVs from 10% to 90%. We measured the intersection throughput, average waiting delays, accrued energy consumption per vehicle (gasoline and electricity), and the associated emission of toxic air pollutants (PM_x, NO_x, CO_2, CO, HC).

The main findings from our work are the following:

- In what concerns the penetration of BEVs and BEAVs, we found the driving profile to be an important factor. BEVs being human-driven, such as ICEVs, have no visible impact in the considered metrics. Conversely, adding more BEAVs generally improves the metrics, except for the energy consumption and under a reactive IM. BEAVs use speed feedback controllers that keep speed steady, leading to higher average speed than BEVs, thus higher energy consumption. The performance of the reactive IMs seems to be close to optimal, not offering further improvements when adding BEAVs. With the other IMs, adding BEAVs increases throughput, reduces waiting time, and causes ICEVs to produce less emissions.

- Among all tested IMs, the reactive ones (SIMP-S and SIMP-D) offer the best performance in all metrics, with a minimal advantage of SIMP-S over SIMP-D. However, these are research protocols that have not yet been implemented practically. The intelligent approaches (ITLC and QTLC) exhibit the second-best performance, with a minimal advantage of ITLC over QTLC, thus seeming a good option when a sensing infrastructure can be deployed. The conventional approaches are infrastructure-free, and TTLC consistently shows better performance than RR, which is why TTLC is more used in practice. The adaptive approaches (MCA and WTLC) offer poor performance, similar to that of RR, seeming unsuited for time-invariant traffic patterns.

In future research, we plan to investigate the toxic emissions generated when producing the electricity consumed by electric vehicles. Additionally, we aim to study transportation sustainability in a city-wide road network and carry out a practical deployment of the SIMP protocol.

CRediT authorship contribution statement

Radha Reddy: Writing – review & editing, Writing – original draft, Investigation, Formal analysis, Data curation, Conceptualization. **Luis Almeida:** Writing – review & editing, Validation, Supervision, Project administration, Formal analysis. **Pedro M. Santos:** Writing – review & editing, Writing – original draft, Validation, Supervision. **Harrison Kurunathan:** Writing – review & editing, Writing – original draft. **Eduardo Tovar:** Supervision, Resources, Project administration, Funding acquisition.

Annex. NO_x, CO_2, CO And HC emissions graphs

See Figs. 11–14.

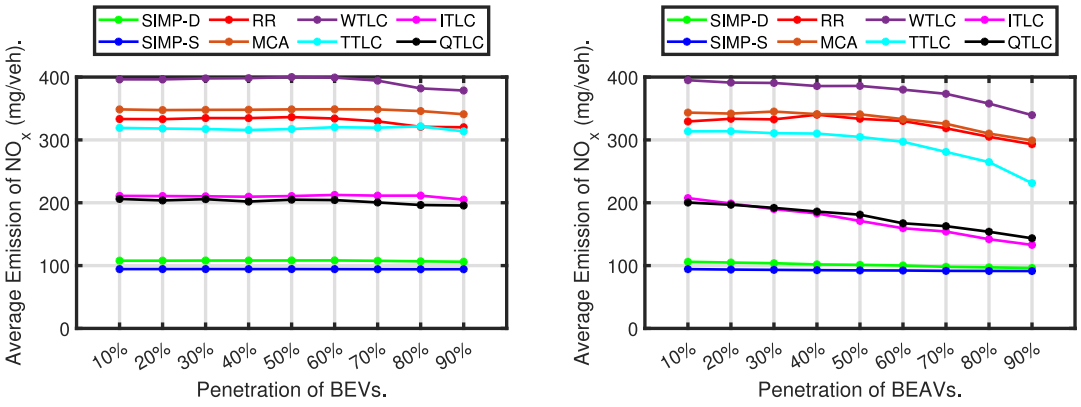

(a) Penetration of BEVs. (b) Penetration of BEAVs.

Fig. 11. Average NO_x emission (mg/veh) per ICEV under various IM approaches and with increasing BEVs and BEAVs.

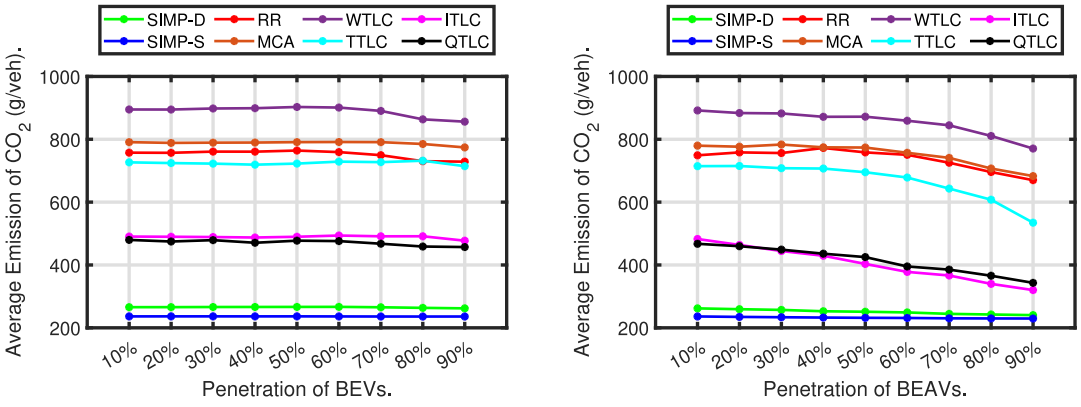

(a) Penetration of BEVs. (b) Penetration of BEAVs.

Fig. 12. Average CO_2 emission (g/veh) per ICEV for various IM approaches at various BEVs and BEAVs penetration ratios.

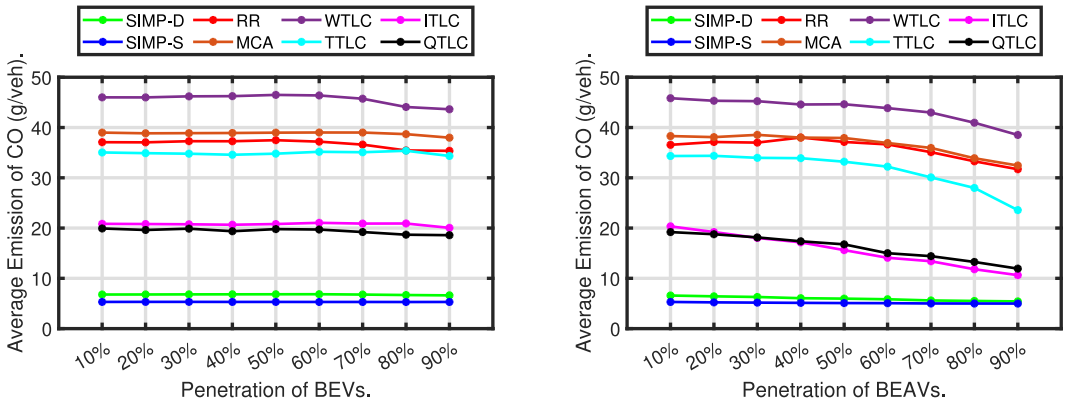

(a) Penetration of BEVs. (b) Penetration of BEAVs.

Fig. 13. Average CO (g/veh) emission per ICEV for various IM approaches at various BEVs and BEAVs penetration ratios.

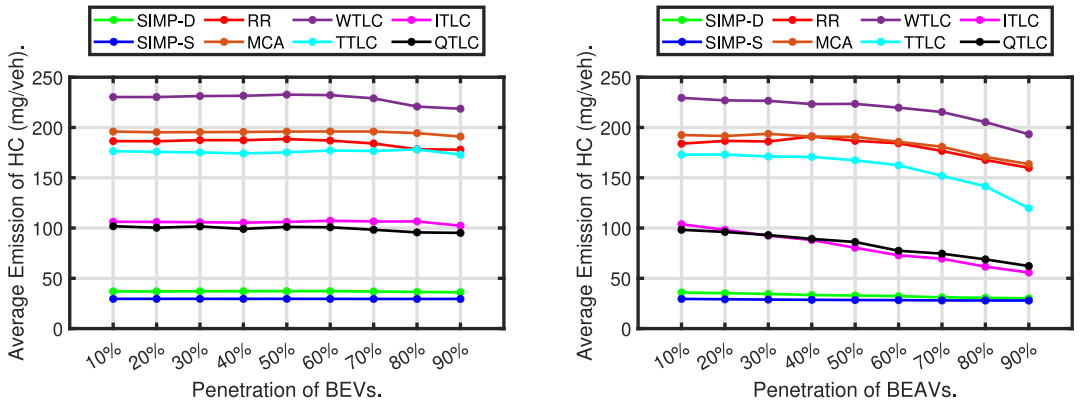

(a) Penetration of BEVs. (b) Penetration of BEAVs.

Fig. 14. Average HC emission (mg/veh) per ICEV for various IM approaches at various BEVs and BEAVs penetration ratios.

References

Abdulhai, B., Pringle, R., Karakoulas, G.J., 2003. Reinforcement learning for true adaptive traffic signal control. J. Transp. Eng. 129 (3).

Ahn, K., Du, J., Farag, M., Rakha, H.A., 2023. Evaluating an eco-cooperative automated control system. Transp. Res. Rec. 2677 (2), 1562–1578.

Ahn, K., Park, S., Rakha, H.A., 2020. Impact of intersection control on battery electric vehicle energy consumption. Energies 13 (12), 3190.

Alekszejenkó, L., Dobrowiecki, T.P., 2019. SUMO based platform for cooperative intelligent automotive agents. In: SUMO. pp. 107–123.

Alkheir, A.A., Aloqaily, M., Mouftah, H.T., 2018. Connected and autonomous electric vehicles (caevs). IT Professional 20 (6), 54–61.

Athanasopoulou, L., Bikas, H., Stavropoulos, P., 2018. Comparative well-to-wheel emissions assessment of internal combustion engine and battery electric vehicles. Proc. CIRP 78, 25–30.

Bharadwaj, S., Ballare, S., Chandel, M.K., et al., 2017. Impact of congestion on greenhouse gas emissions for road transport in Mumbai metropolitan region. Transp. Res. Proc. 25, 3538–3551.

Bieker, G., 2021. A global comparison of the life-cycle greenhouse gas emissions of combustion engine and electric passenger cars. Communications 49 (30), 847129–102.

Björck, E., Omstedt, F., 2018. A comparison of algorithms used in traffic control systems. Technical Report, KTH Royal Institute Of Technology, pp. 1–38.

Chandler, B.E., Myers, M., Atkinson, J.E., Bryer, T., Retting, R., Smithline, J., Trim, J., Wojtkiewicz, P., Thomas, G.B., Venglar, S.P., et al., 2013. Signalized intersections informational guide. Technical Report, United States. Federal Highway Administration. Office of Safety.

Chen, H., Rakha, H.A., 2022. A smart city signalized ECO-cooperative adaptive cruise control and multi-objective dynamic routing system. In: 2022 IEEE International Conference on Smart Mobility. SM, IEEE, pp. 38–45.

Choudhary, A., Gokhale, S., 2016. Urban real-world driving traffic emissions during interruption and congestion. Transp. Res. D: Transp. Environ. 43, 59–70.

Das, S., Boruah, A., Banerjee, A., Raoniar, R., Nama, S., Maurya, A.K., 2021. Impact of COVID-19: A radical modal shift from public to private transport mode. Transp. Policy 109, 1–11.

Dong, H., Zhuang, W., Chen, B., Wang, Y., Lu, Y., Liu, Y., Xu, L., Yin, G., 2022. A comparative study of energy-efficient driving strategy for connected internal combustion engine and electric vehicles at signalized intersections. Appl. Energy 310, 118524.

Faria, R., Moura, P., Delgado, J., De Almeida, A.T., 2012. A sustainability assessment of electric vehicles as a personal mobility system. Energy Convers. Manage. 61, 19–30.

Fuinhas, J.A., Koengkan, M., Leitão, N.C., Nwani, C., Uzuner, G., Dehdar, F., Relva, S., Peyerl, D., 2021. Effect of battery electric vehicles on greenhouse gas emissions in 29 European union countries. Sustainability 13 (24), 13611.

García, A., Monsalve-Serrano, J., Martinez-Boggio, S., Alcaide, R.S., 2023. Carbon footprint of battery electric vehicles considering average and marginal electricity mix. Energy 268, 126691.
Gately, C.K., Hutyra, L.R., Peterson, S., Wing, I.S., 2017. Urban emissions hotspots: Quantifying vehicle congestion and air pollution using mobile phone GPS data. Environ. Pollut. 229, 496–504.
Grossberndt, S., Bartonova, A.G.O., 2021. Public awareness and efforts to improve air quality in europe. Technical Report, EEA and NILU, pp. 1–47.
HCM, 1997. Highway Capacity Manual 2000. (193), Transportation Research Board, National Research Council, pp. 1–1207.
He, X., Wu, X., 2018. Eco-driving advisory strategies for a platoon of mixed gasoline and electric vehicles in a connected vehicle system. Transp. Res. D: Transp. Environ. 63, 907–922.
Helmers, E., Marx, P., 2012. Electric cars: technical characteristics and environmental impacts. Environ. Sci. Eur. 24 (1), 1–15.
Hill, N., Raugei, M., Pons, A., Vasileiadis, N., Ong, H., Casullo, L., 2023. Environmental challenges through the life cycle of battery electric vehicles. Technical Report No. PE 733.112, European Parliament's Committee on Transport and Tourism., pp. 1–83.
Iacobucci, R., McLellan, B., Tezuka, T., 2018. Modeling shared autonomous electric vehicles: Potential for transport and power grid integration. Energy 158, 148–163.
IEA, 2022. Electric vehicles, IEA, Paris, license: CC by 4.0. [Online; accessed 19-May-2023].
Kawamoto, R., Mochizuki, H., Moriguchi, Y., Nakano, T., Motohashi, M., Sakai, Y., Inaba, A., 2019. Estimation of CO2 emissions of internal combustion engine vehicle and battery electric vehicle using LCA. Sustainability 11 (9), 2690.
Keller, M., Hausberger, S., Matzer, C., Wüthrich, P., Notter, B., 2010. Handbook of emission factors for road transport (HBEFA) 3.1. In: Technical Report, Quick Reference. Technical report, INFRAS, pp. 1–76.
Khan, M.A., Sayed, H.E., Malik, S., Zia, T., Khan, J., Alkaabi, N., Ignatious, H., 2022. Level-5 autonomous driving—Are we there yet? A review of research literature. ACM Comput. Surv. 55 (2), 1–38.
Koengkan, M., Fuinhas, J.A., Kazemzadeh, E., Alavijeh, N.K., de Araujo, S.J., 2022. The impact of renewable energy policies on deaths from outdoor and indoor air pollution: Empirical evidence from Latin American and Caribbean countries. Energy 245, 123209.
Koroma, M.S., Costa, D., Philippot, M., Cardellini, G., Hosen, M.S., Coosemans, T., Messagie, M., 2022. Life cycle assessment of battery electric vehicles: Implications of future electricity mix and different battery end-of-life management. Sci. Total Environ. 831, 154859.
Krauß, S., 1998. Microscopic modeling of traffic flow: Investigation of collision free vehicle dynamics. Germany, Dissertation. 115 S 1–129, URL https://elib.dlr.de/8380/, LIDO-Berichtsjahr=1999.
Kurczveil, T., López, P.Á., Schnieder, E., 2013. Implementation of an energy model and a charging infrastructure in SUMO. In: Simulation of Urban MObility User Conference. Springer, pp. 33–43.
Lattanzio, R.K., Clark, C.E., 2020. Environmental effects of battery electric and internal combustion engine vehicles. Technical Report R46420, Congressional Research Service.
Lazaro, O., Robert, E., Lan, L., Gozalvez, J., Turksma, S., Filali, F., Cartolano, F., Urrutia, M., Krajzewicz, D., 2009. iTETRIS: An integrated wireless and traffic platform for real-time road traffic management solutions: D3.1 – traffic modelling: Environmental factors. German Aerospace Center (DLR).
Li, B., Du, H., Li, W., 2016. A potential field approach-based trajectory control for autonomous electric vehicles with in-wheel motors. IEEE Trans. Intell. Transp. Syst. 18 (8), 2044–2055.
Liu, X., Elgowainy, A., Vijayagopal, R., Wang, M., 2020. Well-to-wheels analysis of zero-emission plug-in battery electric vehicle technology for medium-and heavy-duty trucks. Environ. Sci. Technol. 55 (1), 538–546.
Lopez, P.A., Behrisch, M., Bieker-Walz, L., Erdmann, J., Flötteröd, Y.-P., Hilbrich, R., Lücken, L., Rummel, J., Wagner, P., Wieß ner, E., 2018. Microscopic traffic simulation using sumo. In: 2018 21st International Conference on Intelligent Transportation Systems. ITSC, IEEE, pp. 2575–2582.
Lu, C., Dong, J., Hu, L., 2019. Energy-efficient adaptive cruise control for electric connected and autonomous vehicles. IEEE Intell. Transp. Syst. Mag. 11 (3), 42–55.
Mamarikas, S., Doulgeris, S., Samaras, Z., Ntziachristos, L., 2022. Traffic impacts on energy consumption of electric and conventional vehicles. Transp. Res. D: Transp. Environ. 105, 103231.
Marmaras, C., Xydas, E., Cipcigan, L., 2017. Simulation of electric vehicle driver behaviour in road transport and electric power networks. Transp. Res. C 80, 239–256.
Middela, M.S., Mahesh, S., Kancharla, S.R., Ramadurai, G., Perme, R., Sripada, S.K., Devi, G., 2022. Complete LCA of battery electric and conventional fuel vehicles for freight trips. Transp. Res. D: Transp. Environ. 110, 103398.
Milanés, V., Shladover, S.E., 2014. Modeling cooperative and autonomous adaptive cruise control dynamic responses using experimental data. Transp. Res. C 48, 285–300.
Patella, S., Scrucca, F., Asdrubali, F., Carrese, S., 2019. Carbon footprint of autonomous vehicles at the urban mobility system level: A traffic simulation-based approach. Transp. Res. D: Transp. Environ. 74, 189–200.
Ramírez-Díaz, A.J., Ramos-Real, F.J., Barrera-Santana, J., 2023. Well-to-wheels for light-duty vehicle powertrains by segments in isolated systems. Energies 16 (3), 1018.
Reddy, R., Almeida, L., Gaitán, M.G., Santos, P.M., Tovar, E., 2020. Impact of intersection management on energy-efficiency when mixing electric and combustion vehicles. In: 23rd EURO Working Group on Transportation Meeting. pp. 1–3.
Reddy, R., Almeida, L., Gaitan, M., Santos, P., Tovar, E., 2023a. Synchronous management of mixed traffic at signalized intersections towards sustainable road transportation. IEEE Access 11, 64928–64940.
Reddy, R., Almeida, L., Santos, P., Tovar, E., 2023b. Waiting time analysis for a network of signalized intersections. Procedia Comput. Sci. 220, 503–510.
Sadeghi, M., Erol-Kantarci, M., Mouftah, H.T., 2020. Connected and autonomous electric vehicle charging infrastructure integration to microgrids in future smart cities. In: Connected and Autonomous Vehicles in Smart Cities. CRC Press, pp. 1–17.
Sheng, M.S., Sreenivasan, A.V., Sharp, B., Du, B., 2021. Well-to-wheel analysis of greenhouse gas emissions and energy consumption for electric vehicles: A comparative study in Oceania. Energy Policy 158, 112552. http://dx.doi.org/10.1016/j.enpol.2021.112552.
Singh, R., Kumar, A., Singh, A.R., Naidoo, R., Bansal, R.C., Kumar, P., 2019. Environmental feasibility of incorporation of electric taxis in South Africa. J. Eng. 2019 (18), 5078–5084.
UN, WHO, 2016. Ambient air pollution: A global assessment of exposure and burden of disease. World Health Organization 121.
Varaiya, P., 2013. Max pressure control of a network of signalized intersections. Transp. Res. C 36, 177–195.
Verma, S., Dwivedi, G., Verma, P., 2022. Life cycle assessment of electric vehicles in comparison to combustion engine vehicles: A review. Mater. Today: Proc. 49, 217–222. http://dx.doi.org/10.1016/j.matpr.2021.01.666.
Watabe, A., Leaver, J., 2023. Transitioning to battery electric vehicles in Japan: Impact of promotion policy, battery performance and carbon neutrality on greenhouse gas emissions reduction. J. Clean. Prod. 430, 139680.
Webster, F., 1958. Traffic Signal Settings, Road Research Technical Paper No. 39. Road Research Laboratory.
WHO, 2022. World health statistics 2022: monitoring health for the SDGs, sustainable development goals. World Health Organization, pp. 1–131.
Xiao, L., Wang, M., Van Arem, B., 2017. Realistic car-following models for microscopic simulation of adaptive and cooperative adaptive cruise control vehicles. Transp. Res. Rec. 2623 (1), 1–9.
Younes, M.B., Boukerche, A., 2014. An intelligent traffic light scheduling algorithm through VANETs. In: 39th Annual IEEE Conference on Local Computer Networks Workshops. IEEE, pp. 637–642.

Zhang, Y., Ai, Z., Chen, J., You, T., Du, C., Deng, L., 2021a. Energy-saving optimization and control of autonomous electric vehicles with considering multiconstraints. IEEE Trans. Cybern. 10869–10881.

Zhang, J., Tang, T.-Q., Yan, Y., Qu, X., 2021b. Eco-driving control for connected and automated electric vehicles at signalized intersections with wireless charging. Appl. Energy 282, 116215.

Zhao, H.-X., He, R.-C., Yin, N., 2021. Modeling of vehicle CO2 emissions and signal timing analysis at a signalized intersection considering fuel vehicles and electric vehicles. Eur. Transp. Res. Rev. 13 (1), 1–15.